Phase Behavior and Morphological Characteristics of Compositionally Symmetric Diblock Copolymer Blends

Lisaleigh Kane,[†] Michael M. Satkowski,[‡] Steven D. Smith,[*,‡] and Richard J. Spontak[*,†]

Department of Materials Science & Engineering, North Carolina State University, Raleigh, North Carolina 27695, and Corporate Research Division, The Procter & Gamble Company, Cincinnati, Ohio 45239

Received September 9, 1996[⊗]

ABSTRACT: Recent experimental and theoretical efforts suggest that ordered diblock copolymer blends can be approximated as single-component systems of average composition or molecular weight (or both) if the constituent copolymers are closely matched with respect to composition and molecular weight. In this work, we explore the phase behavior and morphological characteristics of five series of poly(styrene-*b*-isoprene) (SI) diblock copolymer blends in which all of the constituent copolymers are compositionally symmetric (50/50 w/w S/I) so that only copolymer molecular weight disparity is varied. Every blend consists of a copolymer with a number-average molecular weight of 120 000 and a second copolymer with a molecular weight between 12 000 and 68 000. Transmission electron microscopy (TEM) and small-angle X-ray scattering (SAXS) have been performed to identify the phase(s) present, as well as to quantitate lamellar spacings and phase compositions as functions of blend composition, in each series. Results obtained from both techniques are in reasonably favorable agreement with each other and with predictions from a theoretical formalism proposed for strongly segregated lamellar diblock copolymer blends.

Introduction

Control over the microstructure present in ordered block copolymers can be of considerable importance in both fundamental studies and commercial applications. Block copolymers are composed of at least two long contiguous monomer sequences and microphase-order into a variety of periodic microstructures if the sequences are incompatible. Early morphological and phase studies of block copolymers relied almost exclusively on model materials tailored with respect to composition and molecular weight through careful chemical synthesis.[1−3] Later efforts demonstrated that copolymer morphology and microstructural dimensions could be precisely adjusted at nanometer length scales through the addition of either a parent[4−7] or block-preferential[8−10] homopolymer of sufficiently low molecular weight relative to that of the host copolymer block. In the presence of such a homopolymer, an ordered block copolymer exhibits either microdomain swelling, a morphological (order-order) transition, or macrophase separation, depending on both the homopolymer molecular weight and concentration. These results have been used in conjunction with theoretical frameworks to estimate the spatial distribution of microdomain-incorporated homopolymer,[11,12] as well as to identify morphology and phase boundaries.[13]

Since the classic study of Hadziioannou and Skoulios,[14] few published works have addressed the phase and morphological characteristics of binary diblock copolymer/copolymer blends until recently. Over the past few years, much experimental[15−18] and theoretical interest[19−22] has grown up around $(AB)_\alpha/(AB)_\beta$ blends composed of α and β AB diblock copolymers differing in morphology (composition). Such copolymer blends provide a practical means by which to not only produce single-phase copolymer systems possessing intermediate, and sometimes "nonclassical" (e.g., gyroid[17,24−26] or hexagonally perforated lamellar[6,7,27,28]) morphologies, but also to elucidate the effect of mixing grafted chains differing in size on local packing[29] and, hence, interfacial curvature in molecularly constrained systems. In a series of related studies[30] addressing $(AB)_\alpha/(AB)_\beta$ blends, the molecular weight, as well as compositional, disparity of the constituent copolymers has been varied to probe intramicrodomain block packing and phase miscibility. Both experimental evidence[30] and theoretical predictions[22] have shown that, beyond a critical molecular weight ratio, the copolymers comprising the blend demix into two phases, one α-rich and the other β-rich.

In this work, we employ transmission electron microscopy (TEM) and small-angle X-ray scattering (SAXS) to examine and compare the morphologies and phase behavior of five different series of $(AB)_\alpha/(AB)_\beta$ blends composed of symmetric diblock copolymers. By maintaining constant composition, the effect of molecular weight alone on blend characteristics is discerned. Experimental results obtained here are quantitatively compared to predictions from theoretical formalisms developed[21,22] for strongly segregated lamellar diblock copolymer blends.

Experimental Section

I. Materials. Six poly(styrene-*b*-isoprene) (SI) diblock copolymers were synthesized via living anionic polymerization with *sec*-butyllithium in cyclohexane at 60 °C. According to proton nuclear magnetic resonance (^{1}H NMR) spectroscopy, the styrene weight fraction (w_S) of these copolymers was constant at 0.50. From gel permeation chromatography (GPC), the copolymers possessed number-average molecular weights ($\bar{M}_n$'s) ranging from 12 000 to 120 000 and reasonably low polydispersities ($\leq$1.05). To facilitate blend descriptions, these copolymers are hereafter designated as SIx, where x, defined as $\bar{M}_n$/1000, can assume the following values: 12, 24, 40, 54, 68, and 120. The molecular characteristics of these parent copolymers are listed in Table 1.

II. Methods. Physical blends of the SI120 (α) copolymer with each of the remaining (β) copolymers were prepared in typically 20 wt % increments from pure α to pure β by dissolving predetermined masses of each copolymer in toluene

* Authors to whom correspondence should be addressed.
† North Carolina State University.
‡ The Procter and Gamble Company.
⊗ Abstract published in *Advance ACS Abstracts,* December 1, 1996.

S0024-9297(96)01329-0 CCC: $12.00

Table 1. Molecular and Microstructural Characteristics of the Parent Copolymers Employed Here

			D (nm)		
designation	w_S[a]	$\bar{M}_n$[b]	SAXS[c]	FT-TEM[d]	$\bar{\epsilon}$[e]
α copolymer					
SI120	0.50	120 000	64.5	64.0(3.7)	
β copolymers					
SI12	0.50	12 000			0.10
SI2	0.50	24 000	20.5	20.9(1.3)	0.20
SI40	0.50	40 000	28.0	29.2(1.8)	0.33
SI54	0.50	54 000	34.5	34.0(2.0)	0.45
SI68	0.50	68 000	40.8	40.6(2.4)	0.57

[a] Measured from ^{1}H NMR. [b] Determined from GPC. [c] Discerned from SAXS patterns (±3% error). [d] Obtained from FT-TEM analysis (standard deviation given in parentheses). [e] Average molecular weight ratio calculated from $\bar{M}_{n,\beta}/\bar{M}_{n,\alpha}$.

at a concentration of 4% (w/v) and casting the solutions into Teflon molds. After slow solvent evaporation over the course of 3 weeks at ambient temperature, the resulting films of the pure copolymers and their blends, measuring about 0.5 mm thick, were annealed at 110 °C (which is above the maximum polystyrene glass transition temperature, T_g^S, of 100 °C) under vacuum for 4 h. Under these conditions, the morphologies produced were presumed to be representative of near-equilibrium.[6,17]

For TEM analysis, the films were microtomed normal to the film surface in a Reichert-Jung Ultracut-S ultramicrotome maintained at −100 °C. Electron-transparent sections were stained with the vapor of 2% OsO_4(aq) for 90 min and imaged on a Zeiss EM902 electron spectroscopic microscope operated at 80 kV and $\Delta E = 50-120$ eV. Negatives were digitized, and the digital images were Fourier-transformed using Digital-micrograph software (Gatan Inc., Pleasanton, CA) to deduce microdomain periodicities from the positions of correlation maxima in Fourier space. Small-angle X-ray scattering was performed on bulk films with Cu Kα radiation ($\lambda = 0.154$ nm) from a Rigaku RU-300 rotating anode. The generator was operated at 40 kV and 40 mA with a 0.2 × 0.2 mm focal size (a 0.2 × 0.2 mm filament run in point mode). Two-dimensional scattering patterns were collected with a Siemens instrument consisting of the HI-STAR wire detector and Anton Parr HR-PHK collimation system.

Collimation for this system was achieved with a single 100 μm diameter pinhole 490 mm from the focal spot (the size of the focal spot restricts beam divergence). A 300 μm guard pinhole was placed 650 mm from the focal spot, just in front of the sample, and the detector was placed a distance of 650 mm from the sample. Nickel filters were used to eliminate extraneous Kβ radiation. Due to the small beam size and large sample-to-detector distance, 2-D intensity patterns could be obtained with minimal instrumental smearing, in which case smearing corrections were not applied. Samples were cut so that the beam path through each sample was nominally 1 mm and placed in the incident beam with the normals of the film surface perpendicular to the incident beam. All samples exhibited anisotropic scattering attributable to the preferred orientation of lamellar normals perpendicular to the film surface. Most of the 2-D SAXS patterns consisted of diffuse intensity arcs over a limited angular range (less than 30° at half-width). In several cases, however, highly oriented lamellae resulted in patterns reminiscent of layer lines. Since long periods were of primary interest here, the diffuse arc patterns were circularly averaged, while slices normal to the layer lines were intensity-averaged, to obtain plots of scattering intensity as a function of scattering vector (q), where $q = (4\pi/\lambda)\sin(\theta/2)$ and θ denotes scattering angle. All peaks clearly showed integral ordering in q, confirming existence of the lamellar morphology in the ordered copolymers.

Results and Discussion

I. Neat Copolymer Phase Behavior. The lamellar morphology of the α (SI120) copolymer, employed in all of the blends investigated in this work, is evident from both the TEM micrograph and SAXS pattern presented in Figure 1. As in subsequent micrographs, the isoprene-rich regions in Figure 1a appear electron opaque (dark) due to the presence of OsO_4, which preferentially reacts with unsaturated bonds. The SAXS pattern seen in Figure 1b is representative of a compositionally symmetric lamellar copolymer, since only the odd reflections are prominent. Shown for comparison in Figure 1b is an example trace (along the lamellar normal) from the Fourier-transform of a TEM image similar to, but of lower magnification (for improved statistical accuracy) than, the one displayed in Figure 1a. Excellent agreement between odd-order peak positions from the FT-TEM and SAXS data is clearly evident in Figure 1b. Note that since a real-space micrograph is used to generate a reciprocal-space image, the FT-TEM trace exhibits additional maxima corresponding to the even reflections of the lamellar morphology. Microdomain periodicity (D) values reported throughout this study are obtained from data such as those provided in Figure 1b by first deducing the principal (first-order) peak position (q^*) from plots of reflection position *vs* reflection order and then applying Bragg's law ($D = 2\pi/q^*$).

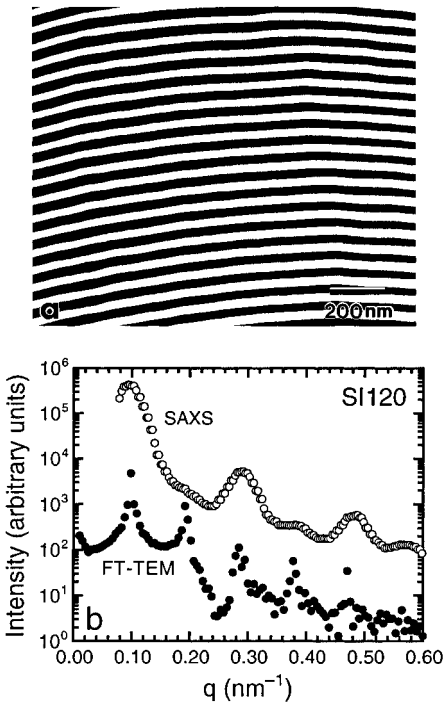

Figure 1. Morphological characteristics of the SI120 (α) copolymer employed in each of the blends examined in this study. In (a), a TEM micrograph illustrates that the symmetric copolymer exhibits alternating lamellae. Isoprene-rich lamellae appear dark due to OsO_4 staining. Shown in (b), the SAXS pattern as well as a trace along the Fourier-transform of an electron micrograph of SI120 both display integral scattering reflections and are representative of the lamellar morphology.

Electron micrographs of the five β copolymers employed in this study are presented in Figure 2. From this series of images, the SI68 (Figure 2a), SI54 (Figure 2b), SI40 (Figure 2c), and SI24 (Figure 2d) copolymers are all clearly microphase-ordered, exhibiting alternating lamellae. In contrast, SI12 is not well-ordered, since only composition fluctuations[3,6] are discernible in Figure 2e. Assignment of segregation regime (weak, intermediate, or strong) to each of these materials requires knowledge of either the scaling behavior of D with $\bar{M}_n$ or the thermodynamic incompatibility (χN, where χ denotes the Flory−Huggins interaction parameter and N is the number of statistical segments per copolymer molecule). Listed in Table 1 and provided on double-

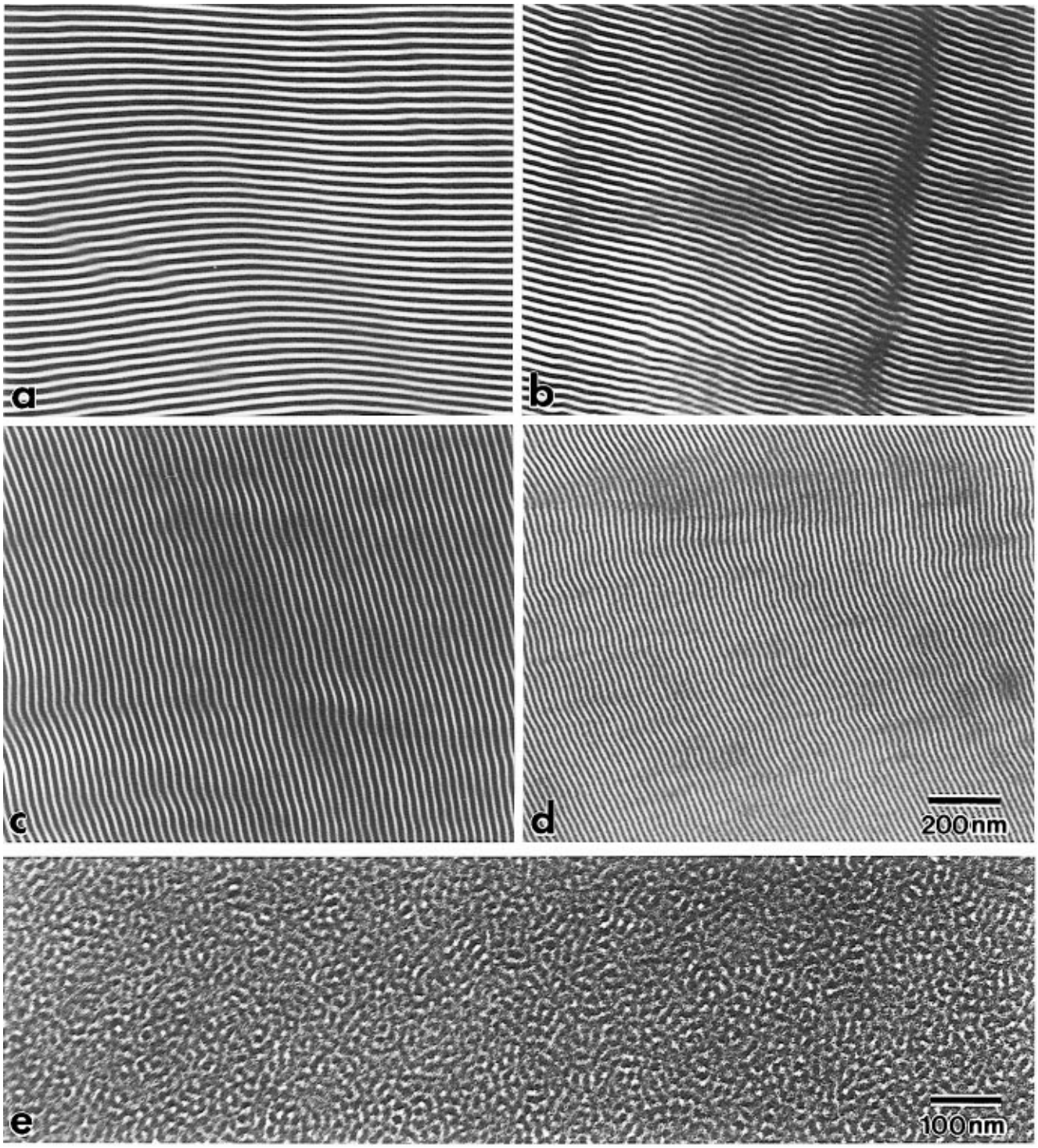

Figure 2. Series of electron micrographs obtained from the neat β copolymers employed in this study: (a) SI68, (b) SI54, (c) SI40, (d) SI24, and (e) SI12. The copolymers seen in (a−d) exhibit the lamellar morphology and are presumed to reside in the intermediate-segregation regime. The SI12 copolymer in (e), displaying composition fluctuations, is weakly segregated.

logarithmic coordinates in Figure 3 are values of D as a function of $\bar{M}_n$ for the neat α and β copolymers, as measured by both SAXS and FT-TEM. From this figure, two characteristics are of particular interest. The first is that D scales as $\bar{M}_n{}^a$, where $a \approx 0.71$. This value of the exponent a is slightly greater than the $^2/_3$ exponent predicted[31] for strongly segregated diblock copolymers (and provided for comparison in Figure 3) and may be due to the ±10% variation in molecular weights, as measured by GPC. A scaling exponent exceeding $^2/_3$ is likewise consistent with predictions[32,33] for the intermediate-segregation regime. Another notable feature of Figure 3 is the close quantitative agreement between SAXS and FT-TEM data, which will become more evident in the section addressing the copolymer blends.

As mentioned above, a second protocol for assignment of copolymer segregation regime relies on the magnitude of χN. From a variable-temperature SAXS study[34] of a symmetric SI diblock copolymer (with $\bar{M}_n = 13\,600$), we estimate χN to be about 86 for SI120 (calculated at $T_g{}^S = 100$ °C) and 11 for SI12 (evaluated at $T_g{}^S \approx 44$ °C[34]). On the basis of the theoretical treatments of Melenkevitz and Muthukumar[32] and, more recently, of Matsen and Bates,[33] χN must exceed ~100 before strong segregation is first realized (other conditions, such as stretched blocks and narrow interfaces, must also be met to fully satisfy the requirements of this regime).

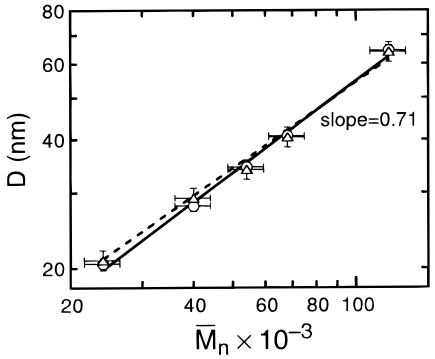

Figure 3. Double-logarithmic representation of microdomain periodicity (D) as a function of molecular weight ($\bar{M}_n$), as determined from SAXS (○) and FT-TEM (△), for the lamellar copolymers shown in Figures 1 and 2. The slope of the solid line (from a best-fit analysis of all the data) is 0.71. Also shown for comparison (dashed line) is a best-fit linear regression with a slope of $^2/_3$.

Accordingly, all of the microphase-ordered copolymers examined here are expected to reside in the intermediate-segregation regime, in agreement with the conclusion reached earlier from the variation of D with $\bar{M}_n$. The SI12 copolymer (Figure 2e), on the other hand, is classified here as weakly segregated since it exhibits both upper and lower T_gs, but its χN is estimated to be less than 12, the predicted[32] crossover point between the weak- and intermediate-segregation regimes. As a point of reference, recall that the order−disorder point in the mean-field ($N \rightarrow \infty$) limit, neglecting critical composition fluctuations, is predicted[35] to occur at $\chi N = 10.495$.

II. Copolymer Blend Phase Behavior. Shown in Figure 4 are SAXS data obtained from blends of the SI120 (α) copolymer with four of the five β copolymers: SI68 (Figure 4a), SI54 (Figure 4b), SI40 (Figure 4c), and SI24 (Figure 4d). In each blend series, the ratio of $\bar{M}_n$ of the β copolymer to that of the α copolymer is designated $\bar{\epsilon}$, so that $\bar{\epsilon}$ varies from 0.57 in Figure 4a to 0.20 in Figure 4d (see Table 1). Blend compositions in most of these figures extend from 0 wt % α (100 wt % β) to 80 wt % α (20 wt % β) in 20 wt % increments. (Note that the SAXS pattern for the SI120 copolymer is not included in any of these figures since it is provided in Figure 1b.) In each of these four series of SAXS patterns, a systematic progression of the principal (first-order), third-order, and, in some cases, fifth-order scattering peak positions from larger to smaller q (reflecting an increase in D) is observed with an increase in the weight percentage of SI120 (W_α) in each blend. Close examination of the data in Figure 4 reveals that none of the SAXS patterns obtained from α/β blends is the result of two superimposed patterns from coexisting lamellar morphologies differing in periodicity (as would be the case upon macrophase separation of the α and β copolymers).

From the SAXS data presented in Figure 4 and the electron micrographs (of some of the SI120/SI68, SI120/SI40, and SI120/SI24 blends) in Figure 5, it can be concluded that all of the blends composed of SI120 and any of the microphase-ordered β copolymers (SI68, SI54, SI40, or SI24) are single-phase at the blend concentrations examined. Even though the molecular weight of the α copolymer is 5 times greater than that of the β copolymer in the SI120/SI24 blend, the results shown here indicate that miscibility is retained in all of these diblock copolymer blends, which is consistent with experimental results reported by Hashimoto et al.[30] In

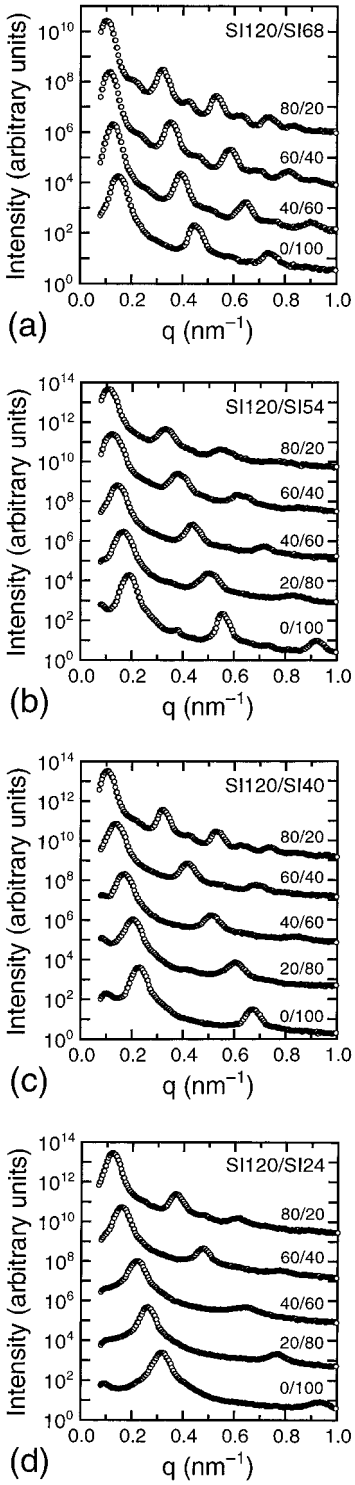

Figure 4. SAXS patterns corresponding to blends of the SI120 (α) diblock copolymer with the microphase-ordered β copolymers: (a) SI68, (b) SI54, (c) SI40, and (d) SI24. Blend compositions are expressed in weight percent of each constituent copolymer.

one of their miscible blends, composed of two copolymers (one lamellar and one bicontinuous cubic) differing in composition by about 21 wt % styrene, the molecular-weight ratio of α to β ($1/\bar{\epsilon}$) was about 5.2. Phase miscibility is also predicted in the present diblock copolymer blends. According to the self-consistent field framework developed by Matsen,[22] macrophase separation occurs in symmetric diblock copolymer blends when $1/\bar{\epsilon} \approx 5.6$, if the chemical incompatibility of the α copolymer (χN_α) is 80 (in the present work, $\chi N_\alpha \approx 86$).

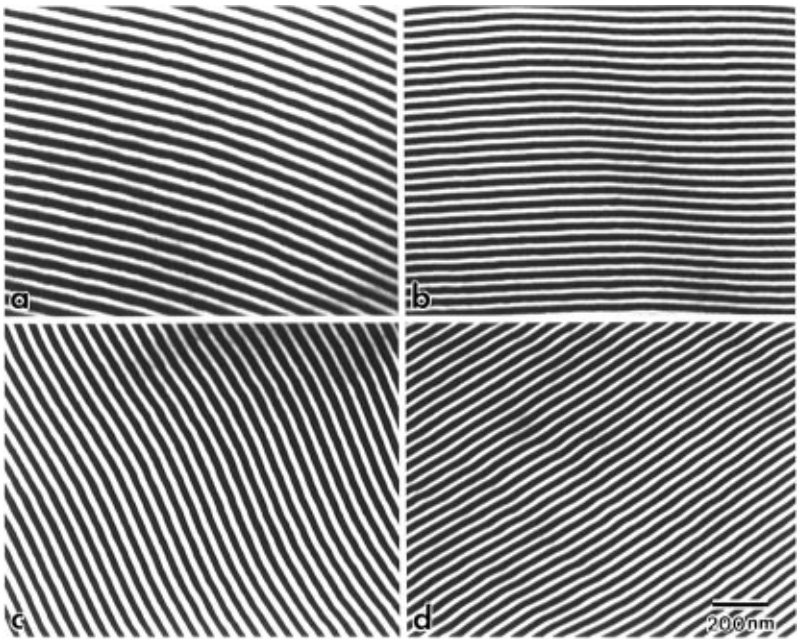

Figure 5. Representative transmission electron micrographs of some of the blends described in Figure 4. All of the miscible blends examined in this study exhibit the lamellar morphology, which is clearly evident in the blends shown here: (a) 80/20 SI120/SI68, (b) 40/60 SI120/SI68, (c) 80/20 SI120/SI40, and (d) 70/30 SI120/SI24. Compositions are expressed in weight percent of each copolymer.

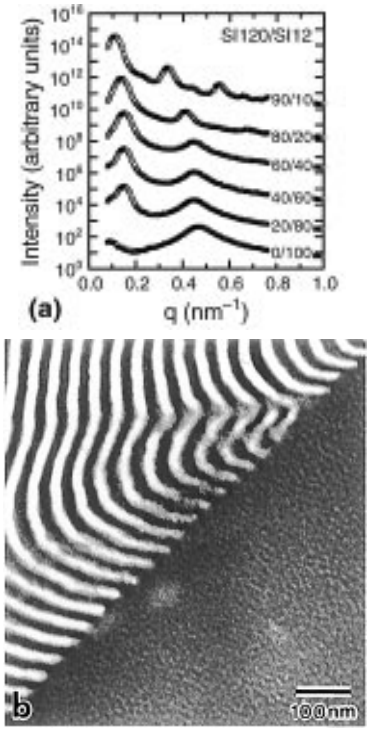

Figure 6. Morphological data collected from the SI120/SI12 blends by (a) SAXS and (b) TEM. Between pure SI12 and 40 wt % SI12, the principal scattering maxima in (a) do not vary appreciably, implying that the SI120 and SI12 copolymers demix. Phase separation is confirmed in the micrograph from the 60/40 SI120/SI12 blend displayed in (b). Blend compositions are expressed in weight percent of each constituent copolymer.

In marked contrast to the results shown in Figures 4 and 5, the SI120/SI12 blend (with $\bar{\epsilon} = 0.10$) appears to be macrophase-separated at some intermediate blend concentrations in both the SAXS patterns displayed in Figure 6a and the electron micrograph presented in Figure 6b. In Figure 6a, the principal scattering maximum of SI12 does not change much (from 0.47 to 0.45 nm^{-1}) despite the variation in blend concentration from pure SI12 to 40 wt % SI12 (60 wt % SI120). Likewise, the principal peak position of the SI120 copolymer in the vicinity of 0.15 nm^{-1} does not differ substantially from 40 to 80 wt % SI12. While the concentration range from 100 to 40 wt % SI12 appears relatively broad, it corresponds to a difference of only about 13 mol% SI12. The electron micrograph seen in Figure 6b clearly provides evidence of phase demixing between the SI120 and SI12 copolymers. In this figure, the SI120-rich regions exhibit alternating lamellae (as in Figure 1a), whereas areas that are relatively featureless are rich in the weakly segregated SI12 copolymer. The evidence provided in Figure 6 of partial blend miscibility in the SI120/SI12 series is again consistent with prior experimental results[30] (although the previously reported blend consisted of one asymmetric lamellar copolymer and one symmetric disordered copolymer), as well as theoretical predictions.[22]

The variation of D with respect to blend composition (W_α) is provided for all of the miscible blend series in Figure 7 and for the partially immiscible SI120/SI12 blend in Figure 8. In addition, the numerical values of D are provided in Table 2 for all of the blends investigated here. As the concentration of SI120 is reduced in any of the blend series shown in Figure 7, D is found to decrease steadily until the periodicity of the pure β copolymer is attained. Spacings obtained from FT-TEM are seen in Figure 7 and Table 2 to be in good quantitative agreement with those measured from SAXS. Such agreement helps to confirm that the stained copolymer sections did not undergo extensive beam damage (as evidenced by noticeable specimen shrinkage) during image acquisition.

In Figure 8, periodicities characteristic of lamellar morphologies are provided for SI120/SI12 blends in the one- and two-phase regions. Correlation lengths (L_c, also measured from the principal scattering peak positions of the SAXS patterns provided in Figure 6) are likewise displayed for weakly segregated (SI12-rich) morphologies. While the L_c values corresponding to the neat SI12 copolymer and SI12-rich phase are virtually independent of W_α, indicating that the SI12-rich phase

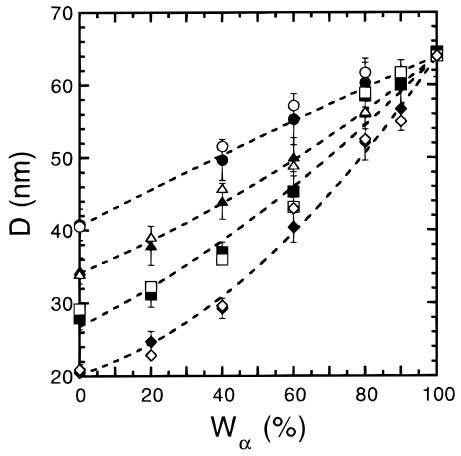

Figure 7. Microdomain periodicities (D) as a function of blend composition (W_α) for all of the miscible blends examined by SAXS (filled symbols) and TEM (open symbols). The β copolymer in each blend series is SI68 (circles), SI54 (triangles), SI40 (squares), and SI24 (diamonds). Vertical lines denote experimental error, and the dashed lines are eye guides for each blend series.

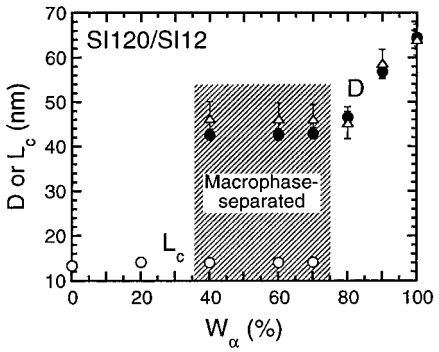

Figure 8. Variation of the lamellar long spacings (D; ● from SAXS, △ from TEM) and weakly segregated correlation lengths (L_c; ○) with blend composition in the SI120/SI12 series. The two-phase region appears cross-hatched, and vertical lines on the data denote experimental error.

does not contain an appreciable fraction of SI120 molecules, the D-spacings for the SI120 copolymer decrease measurably upon addition of SI12. Moreover, the periodicities exhibit a reduced, but relatively constant, plateau within the macrophase-separated region. This reduction in D for the SI120 copolymer with decreasing W_α implies that the SI120-rich phase contains a measurable concentration of SI12 molecules. Such partitioning of the constituent copolymer molecules among the two coexisting phases has been previously observed in the asymmetric copolymer blends studied by Hashimoto et al.[30] and will be analyzed further in the next section.

III. Strong-Segregation Blend Theory. Several theoretical formalisms have been recently proposed[19,23] to predict the binary phase diagram of ordered diblock copolymer blends. In addition, strong-segregation theories[17,21,22] and a self-consistent field theory[22] have also been developed to deduce microstructural characteristics and block distributions in such blends. In this section, we briefly compare the strong-segregation theories described in refs 21 and 22, as well as predictions from both of these theories to the experimental results presented in the preceding section. The illustration displayed in Figure 9 schematically depicts the coresident A (or B) blocks of a blend composed of two diblock copolymers of identical (but not necessarily symmetric) composition in the lamellar morphology. To ascertain the free energy density of the blend (F), only

Table 2. Microstructural Characteristics of the α/β Blends Containing the SI120 (α) Copolymer

		D (nm)		
β copolymer	W_α (%)	SAXS[a]	FT-TEM[b]	L_c[a] (nm)
SI68	40	49.7	51.6(2.8)	
	60	55.3	57.2(3.5)	
	80	60.3	61.7(3.4)	
SI54	20	37.9	39.1(2.7)	
	40	44.0	45.8(2.5)	
	60	50.1	49.0(2.6)	
	80	56.1	56.4(3.3)	
SI40	20	31.2	32.3(1.7)	
	40	37.0	36.0(1.4)	
	60	45.3	43.2(2.8)	
	80	58.5	58.9(4.6)	
	90	60.0	61.7(3.4)	
SI24	20	24.7	22.9(1.4)	
	40	29.3	29.7(1.4)	
	60	40.4	43.0(2.1)	
	80	52.1	52.5(2.5)	
	90	56.7	55.0(3.0)	
SI12	0			13.4
	20			14.2
	40	42.7	46.3(3.8)	14.1
	60	42.7	46.3(3.6)	14.1
	70	43.0	46.2(3.3)	14.2
	80	46.6	45.4(3.6)	
	90	56.9	58.7(3.2)	

[a] Discerned from SAXS patterns (±3% error). [b] Obtained from FT-TEM analysis (standard deviation given in parentheses).

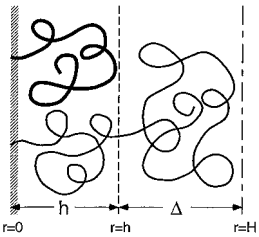

Figure 9. Schematic illustration of a diblock copolymer blend showing half of a single A or B lamella. Shorter β copolymer molecules are restricted to occupy the h layer, while the longer α copolymer molecules reside in both the h and Δ layers comprising H. In this work, the α and β copolymers are restricted to possess identical (but not necessarily symmetric) compositions.

the half-lamellar (H) region shown in Figure 9 is explicitly treated due to symmetry considerations. Here, H is divided into two layers: h, in which the shorter β blocks mix with a generally unspecified fraction of the longer α blocks, and Δ, in which only the unmixed fraction of the α blocks is deposited. As derived elsewhere,[21] the elastic free energy per chain of a single mixed layer (F_h) can be written as

$$\frac{F_h}{kT} = \frac{\pi^2 \sigma h^3}{8b^5(\epsilon N_\alpha)^2} + \frac{3\pi x h^2}{4b^2 \epsilon N_\alpha} \cot\left(\frac{\pi\Gamma}{2\epsilon}\right) \qquad (1)$$

where k is the Boltzmann constant, T denotes absolute temperature, b is the length of a statistical segment, N_α is the number of statistical segments comprising the α copolymer, x is the mole fraction of α, and $\epsilon = N_\beta/N_\alpha$. The parameter Γ defines the fraction of α segments residing in h, and arises from the following conservation of mass constraint:

$$\int_0^h E_\alpha^{-1}(r)\, dr = \Gamma N_\alpha \qquad (2)$$

where $E_\alpha(r)$ is the local free energy of elastic deformation of the stretched α chain along the direction of the lamellar normal (r).

Equation 2 requires that the ΓN_αth segment of each α chain dwells at *h*, since the α units residing in *h* are covalently linked to those in Δ. The corresponding expression for the *β* block restricted to *h* is identical to that of a nonuniformly stretched, single-grafted chain, namely,

$$\int_0^\eta E_\beta^{-1}(r,\eta)\,\mathrm{d}r = \epsilon N_\alpha \tag{3}$$

Following Semenov,[31] the free end of the *β* block does not lie at a single position along *r*. Since the chain is nonuniformly stretched, a distribution of locations along *r* is required to describe the position (*η*) of the free end. It has been suggested[22] that eq 2 is flawed, since it does not account for the distribution of α end units in *h*. One way to correct for this shortcoming is to envision the *β* blocks and the fraction of α blocks in *h* as indistinguishable so that an expression similar to eq 3 can be written for the fraction of α blocks occupying *h*. In this case, $\Gamma = \epsilon$ and eq 1 reduces to

$$\frac{F_\mathrm{h}}{kT} = \frac{\pi^2\sigma h^3}{8b^5(\epsilon N_\alpha)^2} \tag{4}$$

which is analogous to the expression derived[31] for neat end-grafted (diblock) copolymers (recall that these F_h must be multiplied by a factor of 2 since there are two *h* regions per lamella). As shown below, however, eq 2 can be used in its present form without introducing error. Just as the *β* block in *h*, the fraction of the α block in Δ is nonuniformly stretched and fixed at one end. Rather than using the potential derived elsewhere[21] for this layer, we recognize here that F_Δ should be of the same form as eq 4, in which case,

$$\frac{F_\Delta}{kT} = \frac{\pi^2\sigma\Delta^3}{8b^5(1-\epsilon)^2 N_\alpha^2} \tag{5}$$

Melt incompressibility is guaranteed from $h\sigma = \epsilon b^3 N_\alpha$, $\Delta\sigma = x(1-\epsilon)b^3N_\alpha$, and $H\sigma = \mu b^3 N_\alpha$, where *σ* is the surface area of a repeat unit and $\mu = \epsilon + x(1-\epsilon)$. Addition of eqs 4 and 5, followed by substitution of the above incompressibility expressions and algebraic rearrangement, yields

$$\frac{F_i}{kT} = \frac{\pi^2\sigma H_i^3}{4b^5 N_{i,\alpha}^2}\left[\frac{\epsilon + x^3(1-\epsilon)}{\mu^3}\right] \tag{6}$$

where i = A or B and $N_{i,\alpha}$ refers to the number of *i* units along the α copolymer. To facilitate comparison between strong-segregation theories, the entropy of mixing term[21] is neglected here. Defining the composition of both copolymers as $f = N_\mathrm{A}/N$, recognizing that $D = 2H_\mathrm{A}/f$, and dividing the free energy per chain (F) by the volume $D\sigma$ eventually results in the free energy density:

$$\frac{F}{kT} = \frac{\pi^2 D^2[\epsilon + x^3(1-\epsilon)]}{32b^2 N_\alpha^2\mu^3} + \frac{2b}{D}\left(\frac{\chi}{6}\right)^{1/2} \tag{7}$$

It immediately follows upon evaluation of $(\mathrm{d}F/\mathrm{d}D) = 0$ that the microdomain periodicity of a lamellar diblock copolymer blend relative to that of the α copolymer ($D_{\alpha\beta}/D_\alpha$) at equilibrium is given by

$$\frac{D_{\alpha\beta}}{D_a} = \mu[\epsilon + x^3(1-\epsilon)]^{-1/3} \tag{8a}$$

from which F/kT can be rewritten as

$$\frac{F}{kT} = \frac{3}{4\mu}\left(\frac{\pi^2\chi}{3N_\alpha^2}\right)^{1/3}[\epsilon + x^3(1-\epsilon)]^{1/3} \tag{8b}$$

Equations 8a and 8b have been reported by Matsen[22] for strongly segregated diblock copolymer blends.

If, instead of setting $\Gamma = \epsilon$ as above, eqs 1 and 5 are combined and the appropriate substitutions and simplifications are made, the free energy for the *i*th lamella (i = A or B) becomes

$$\frac{F_i}{kT} = \frac{\pi^2\sigma H_\mathrm{i}^3}{4b^5 N_{i,\alpha}^2}\left[\frac{\xi^3}{\mu^3\epsilon^2} + \frac{6x\xi^2}{\pi\mu^3\epsilon}\cot\left(\frac{\pi\Gamma}{2\epsilon}\right) + \frac{\tau^3}{\mu^3(1-\epsilon)^2}\right] \tag{9}$$

where $\xi = x\Gamma + \epsilon(1-x)$ from $h\sigma = \xi b^3 N_\alpha$ and $\tau = x(1-\epsilon)$ from $\Delta\sigma = \tau b^3 N_\alpha$. Thus, F/kT is given by

$$\frac{F}{kT} = \frac{\pi^2 D^2}{32b^2 N_\alpha^2}\left[\frac{\xi^3}{\mu^3\epsilon^2} + \frac{6x\xi^2}{\pi\mu^3\epsilon}\cot\left(\frac{\pi\Gamma}{2\epsilon}\right) + \frac{\tau^3}{\mu^3(1-\epsilon)^2}\right] + \frac{2b}{D}\left(\frac{\chi}{6}\right)^{1/2} \tag{10}$$

Upon evaluation of $(\partial F/\partial D)_\Gamma = 0$, one obtains

$$\frac{D_{\alpha\beta}}{D_\alpha} = \mu\left[\frac{\xi^3}{\epsilon^2} + \frac{6x\xi^2}{\pi\epsilon}\cot\left(\frac{\pi\Gamma}{2\epsilon}\right) + \frac{\tau^3}{(1-\epsilon)^2}\right]^{-1/3} \tag{11a}$$

and

$$\frac{F}{kT} = \frac{3}{4\mu}\left(\frac{\pi^2\chi}{3N_\alpha^2}\right)^{1/3}\left[\frac{\xi^3}{\epsilon^2} + \frac{6x\xi^2}{\pi\epsilon}\cot\left(\frac{\pi\Gamma}{2\epsilon}\right) + \frac{\tau^3}{(1-\epsilon)^2}\right]^{1/3} \tag{11b}$$

Evaluation of $(\partial F/\partial\Gamma)_D = 0$ from eq 10 must be performed numerically and produces a very interesting result, namely, $\Gamma = \epsilon$, in which case eqs 11a and 11b collapse to eqs 8a and 8b, respectively. Thus, if the elastic free energy of the α units residing in the Δ layer is treated independently of that describing the α units in the *h* layer (as above), then the strong-segregation theories reported earlier[21,22] are not only equivalent but also require that the number of (indistinguishable) α and *β* units occupying *h* must be identical at equilibrium. [The one remaining difference between the two approaches involves the spatial distribution of α units occupying *h*, but this consideration has no impact on either F or $D_{\alpha\beta}$.]

Since the quantity $D_{\alpha\beta}/D_\alpha$ is a function of only *x* and *ϵ* and is independent of parent copolymer material characteristics (e.g., *χ*), we elect to use this quantity when comparing theoretical predictions to experimental data. It is important to recognize that the shape of the $D_{\alpha\beta}/D_\alpha(x)$ curve is dictated solely by *ϵ*. Shown in Figure 10 is the variation of $D_{\alpha\beta}/D_\alpha$ (average values from SAXS and FT-TEM) with composition W_α (=$100x/\mu$) for each of the fully miscible blend series examined here: SI120/SI68 (Figure 10a), SI120/SI54 (Figure 10b), SI120/SI40 (Figure 10c), and SI120/SI24 (Figure 10d). Also shown in each of these figures are predictions from eq 8a for strongly segregated diblock copolymer blends. Recall that *ϵ* depends on the molecular weights of the α and *β* copolymers and that the accepted uncertainty in $\bar{M}_\mathrm{n}$ values measured by GPC is ±10%. To account for such variation in these comparisons, the *ϵ* used in eq 8a is ascertained from the experimental value of $D_{\alpha\beta}/D_\alpha$ evaluated (by SAXS) at $W_\alpha = 0\%$. Each *ϵ* chosen in this

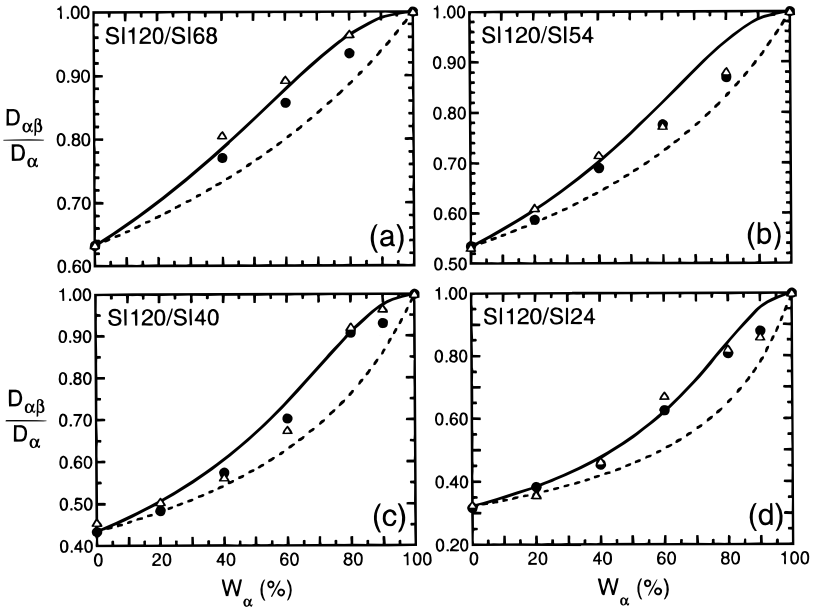

Figure 10. Dependence of the reduced microdomain periodicity ($D_{\alpha\beta}/D_\alpha$) on blend composition (W_α) as discerned from SAXS (●) and FT-TEM (△) for each of the four miscible blend series: (a) SI120/SI68, (b) SI120/SI54, (c) SI120/SI40, and (d) SI120/SI24. Curves are predictions from the strong-segregation blend theory (solid) and the average molecular weight correlation[30] (dashed).

Table 3. Values of ϵ Used to Produce the Theoretical Predictions Displayed in Figure 10

β copolymer	$\bar{\epsilon}$	ϵ_{min}[a]	ϵ_{max}[b]	ϵ
SI24	0.20	0.16	0.24	0.18
SI40	0.33	0.27	0.41	0.29
SI54	0.45	0.37	0.55	0.39
SI68	0.57	0.46	0.69	0.50

[a] Calculated from $(0.9\bar{M}_{n,\beta})/(1.1\bar{M}_{n,\alpha})$ [b] Calculated from $(1.1\bar{M}_{n,\beta})/(0.9\bar{M}_{n,\alpha})$

fashion is then compared to the range of ϵ calculated to account for the ±10% variation in $\bar{M}_n$ in the corresponding copolymer pair.

Selected ϵ values and permissible ϵ ranges are provided in Table 3 for the four blend series examined here and reveal that the ϵ employed in the predictions shown in Figure 10 all lie within acceptable limits. It is interesting to note that these ϵ are all consistently less (by 10−13%) than the $\bar{\epsilon}$ listed in Table 1. Also shown in Figure 10 are predictions from the mean blend molecular weight ($\bar{M}_{n,\alpha\beta}$) correlation proposed by Hashimoto et al.[30] According to this correlation, $D_{\alpha\beta}/D_\alpha$ is conveniently given by $\mu^{2/3}$. Note that, once ϵ is selected, both predicted $D_{\alpha\beta}/D_\alpha(W_\alpha)$ curves must pass through unity at $W_\alpha = 100\%$ and the experimental value of $D_{\alpha\beta}/D_\alpha$ at $W_\alpha = 0\%$. Generally speaking, the strong-segregation blend predictions are seen to be in closer quantitative agreement with the data presented for each of the four miscible diblock copolymer blends in Figure 10 than those obtained from the $\bar{M}_{n,\alpha\beta}$ correlation.[30] Similar agreement has been demonstrated earlier[17,21] for blends in which the constituent copolymers do not possess identical compositions.

Figure 11 shows the variation of $D_{\alpha\beta}/D_\alpha$ with W_α for the partially miscible SI120/SI12 blend series. Since SI12 is weakly segregated, ϵ is taken to equal $\bar{\epsilon}$ (0.10 from Table 1), and the agreement between strong-segregation predictions and experimental data is once again found to be favorable for single-phase SI120/SI12 blends. According to Figures 10 and 11, the $D_{\alpha\beta}/D_\alpha$ values from the $\bar{M}_{n,\alpha\beta}$ correlation[30] consistently underpredict the experimental data for such blends. As alluded to earlier, $D_{\alpha\beta}/D_\alpha$ is measurably less than unity (by as much as ≈34%) in the phase-demixed regime,

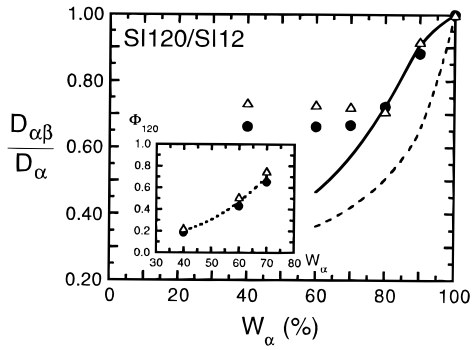

Figure 11. $D_{\alpha\beta}/D_\alpha$ as a function of W_α for the partially miscible SI120/SI12 blend series. The symbols and curves are the same as those described in the caption of Figure 10. The inset shows the fraction of the SI120-rich phase (Φ_{120}) in the three immiscible SI120/SI12 blends as a function of W_α (the dotted line is a guide for the eye).

indicating that a finite fraction of SI12 molecules reside within the SI120-rich phase. The fraction of SI120 molecules (x) comprising the SI120-rich phase is estimated, from $D_{\alpha\beta}/D_\alpha$ (using eq 8a), to average between 0.25 (SAXS) and 0.29 (FT-TEM).

According to Figure 6 and the expanded series of SAXS patterns provided in Figure 12, the correlation length of SI12 in the SI12-rich phase is seen to remain virtually unaffected by the presence of SI120, suggesting that only a small fraction of SI120 molecules are accommodated by the weakly segregated SI12 molecules. If the parent SI12 copolymer and SI12-enriched phases are presumed to be weakly segregated, their correlation lengths are predicted[33] to scale as $\bar{M}_{n,\alpha\beta}^{0.994}$. Analysis of the variation in SI12 correlation length with blend composition in the immiscible SI120/SI12 blends using this scaling relationship reveals that the fraction of SI120 molecules residing in the SI12-rich phase is only about 0.01. Since the blend composition is known ($W_\alpha = 100x/\mu$), as are the compositions of the two coexisting phases, it is possible to calculate the fraction of SI120 phase (Φ_{120}) in each of the phase-separated blends. Estimates of Φ_{120} for the three immiscible SI120/SI12 blends are provided as a function of blend composition in the inset of Figure 11 and are seen to

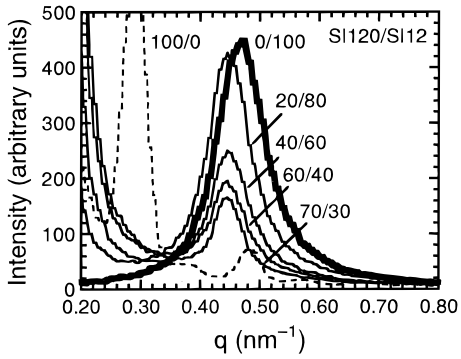

Figure 12. Expanded view of the SAXS patterns from the SI120/SI12 series to more clearly illustrate the invariance of the SI12-rich principal scattering peak (which yields L_c) with blend composition. Patterns from the SI120 and SI12 copolymers are displayed as dashed and bold solid lines, respectively, while SI120/SI12 blends are listed by composition (in weight percent of each copolymer).

increase with increasing W_α. This observed trend is consistent with intuitive expectation, since single-phase (SI120-rich) behavior is recovered at $W_\alpha \approx 80\%$.

Conclusions

Diblock copolymer blends provide an alternative, and attractive, means by which to generate microphase-ordered systems with controlled morphological characteristics and, hence, properties. In this work, we have investigated five series of such blends in which composition remains invariant, so that the effect of molecular weight disparity on blend phase behavior and morphology could be isolated. Microdomain periodicities of the neat copolymers and their blends have been measured by SAXS and FT-TEM and are found to be in favorable quantitative agreement (typically within a few percent difference). The two strong-segregation theories previously proposed[21,22] for diblock copolymer blends are shown to yield identical results without oversimplifying initial assumptions and render predictions that are generally in better agreement with experimental data than those from the average blend molecular weight correlation.[30] While complete miscibility is retained when the ratio of the average molecular weights of the two copolymers comprising the blend is as low as 0.20, phase demixing occurs when this ratio is reduced to about 0.10. Estimates of the coexisting phase compositions (from measured variations in periodicities or correlation lengths) can be used to assess the amount of each phase present in the blend, which is the requisite first step to establishing an experimental phase diagram for such complex blends.

Acknowledgment. This study has been supported by the Petroleum Research Fund, administered by the American Chemical Society; the Shell Development Co.; and the Director, Office of Energy Research, Office of Basic Energy Sciences, Materials Science Division of the U.S. Department of Energy, under contract DE-AC03-76SF00098. R.J.S. thanks the National Center for Electron Microscopy for a Visiting Scientist Fellowship, and L.K. acknowledges support from a GAANN fellowship. We also thank Mr. J. H. Laurer (NCSU) and Mr. J. T. Grothaus (P&G) for technical assistance.

References and Notes

(1) Legge, N. R., Holden, G., Schroeder, H. E., Eds. *Thermoplastic Elastomers: A Comprehensive Review*; Hanser: New York, 1987.
(2) Bates, F. S.; Fredrickson, G. H. *Annu. Rev. Phys. Chem.* **1990**, *41*, 525.
(3) See, for example: Khandpur, A. K.; Förster, S.; Bates, F. S.; Hamley, I. W.; Ryan, A. J.; Bras, W.; Almdal, K.; Mortensen, K. *Macromolecules* **1995**, *28*, 8796.
(4) Hashimoto, T.; Tanaka, H.; Hasegawa, H. *Macromolecules* **1990**, *23*, 4378. Tanaka, H.; Hasegawa, H.; Hashimoto, T. *Macromolecules* **1991**, *24*, 240. Han, C. D.; Baek, D. M.; Kim, J.; Kimishima, K.; Hashimoto, T. *Macromolecules* **1992**, *25*, 3052.
(5) Winey, K. I.; Thomas, E. L.; Fetters, L. J. *Macromolecules* **1991**, *24*, 6182; **1992**, *25*, 422, 2645. Winey, K. I.; Thomas, E. L.; Fetters, L. J. *J. Chem. Phys.* **1991**, *95*, 9367.
(6) Spontak, R. J.; Smith, S. D.; Ashraf, A. *Macromolecules* **1993**, *26*, 956.
(7) Disko, M. M.; Liang, K. S.; Behal, S. K.; Roe, R.-J.; Jeon, K. J. *Macromolecules* **1993**, *26*, 2983.
(8) Tucker, P. S.; Barlow, J. W.; Paul, D. R. *Macromolecules* **1988**, *21*, 1678, 2794.
(9) Hashimoto, T.; Kimishima, K.; Hasegawa, H. *Macromolecules* **1991**, *24*, 5704.
(10) Xie, R.; Yang, B.; Jiang, B. *Macromolecules* **1993**, *26*, 7097.
(11) Banaszak, M.; Whitmore, M. D. *Macromolecules* **1992**, *25*, 2757.
(12) Shull, K. R.; Winey, K. I. *Macromolecules* **1992**, *25*, 2637.
(13) Matsen, M. W. *Macromolecules* **1995**, *28*, 5765.
(14) Hadziioannou, G.; Skoulios, A. *Macromolecules* **1982**, *15*, 267.
(15) Vilesov, A. D.; Floudas, G.; Pakula, T.; Melenevskaya, E. Yu.; Birshtein, T. M.; Lyatskaya, Yu. V. *Macromol. Chem. Phys.* **1994**, *195*, 2317.
(16) Zhao, J.; Majumdar, B.; Schulz, M. F.; Bates, F. S.; Almdal, K.; Mortensen, K.; Hajduk, D. A.; Gruner, S. M. *Macromolecules* **1996**, *29*, 1204.
(17) Spontak, R. J.; Fung, J. C.; Braunfeld, M. B.; Sedat, J. W.; Agard, D. A.; Kane, L.; Smith, S. D.; Satkowski, M. M.; Ashraf, A.; Hajduk, D. A.; Gruner, S. M. *Macromolecules* **1996**, *29*, 4494.
(18) Schulz, M. F. Ph.D. Dissertation, University of Minnesota, 1994.
(19) Shi, A.-C.; Noolandi, J. *Macromolecules* **1994**, *27*, 2936. Shi, A.-C.; Noolandi, J.; Hoffmann, H. *Macromolecules* **1994**, *27*, 6661.
(20) Dan, N.; Safran, S. A. *Macromolecules* **1994**, *27*, 5766.
(21) Spontak, R. J. *Macromolecules* **1994**, *27*, 6363.
(22) Matsen, M. W. *J. Chem. Phys.* **1995**, *103*, 3268.
(23) Matsen, M. W.; Bates, F. S. *Macromolecules* **1995**, *28*, 7298.
(24) Hajduk, D. A.; Harper, P. E.; Gruner, S. M.; Honeker, C. C.; Kim, G.; Thomas, E. L.; Fetters, L. J. *Macromolecules* **1994**, *27*, 4063. Hajduk, D. A.; Harper, P. E.; Gruner, S. M.; Honeker, C. C.; Thomas, E. L.; Fetters, L. J. *Macromolecules* **1995**, *28*, 2570.
(25) Schulz, M. F.; Bates, F. S.; Almdal, K.; Mortensen, K. *Phys. Rev. Lett.* **1994**, *73*, 86.
(26) Laurer, J. H.; Fung, J. C.; Hajduk, D. A.; Smith, S. D.; Gruner, S. M.; Sedat, J. W.; Agard, D. A.; Spontak, R. J. *Macromolecules*, submitted.
(27) Thomas, E. L.; Anderson, D. M.; Henkee, C. S.; Hoffman, D. *Nature* **1988**, *334*, 598.
(28) Hamley, I. W.; Koppi, K. A.; Rosedale, J. H.; Bates, F. S.; Almdal, K.; Mortensen, K. *Macromolecules* **1993**, *26*, 5959. Förster, S.; Khandpur, A. K.; Zhao, J.; Bates, F. S.; Hamley, I. W.; Ryan, A. T.; Bras, W. *Macromolecules* **1994**, *27*, 6922.
(29) Birshtein, T. M.; Lyatskaya, Yu. V.; Zhulina, E. B. *Polymer* **1990**, *31*, 2185. Zhulina, E. B.; Birshtein, T. M. *Polymer* **1991**, *32*, 1299.
(30) Hashimoto, T.; Yamasaki, K.; Koizumi, S.; Hasegawa, H. *Macromolecules* **1993**, *26*, 2895.
(31) Semenov, A. N. *Sov. Phys. JETP (Engl. Transl.)* **1985**, *61*, 731.
(32) Melenkevitz, J.; Muthukumar, M. *Macromolecules* **1991**, *24*, 4199.
(33) Matsen, M. W.; Bates, F. S. *Macromolecules* **1996**, *29*, 1091.
(34) Hong, S.-U.; Lauren, J. H.; Hajduk, D. A.; Smith, S. D.; Duda, J. L.; Spontak, R. J. *Macromolecules*, manuscript in preparation.
(35) Leibler, L. *Macromolecules* **1980**, *13*, 1602.

MA9613291